

## Enhanced and frequency-selectable terahertz emission from two crossed air-plasmas

Mingxin Gao<sup>1,2,\*</sup>, Xing Xu,<sup>1</sup> Jing Lou,<sup>1</sup> Ruixing Wang,<sup>1</sup> Ziyi Zhang<sup>1</sup>, Zhijin Wen,<sup>3,†</sup>  
Chao Chang<sup>1,4,‡</sup> and Yindong Huang<sup>1,§</sup><sup>1</sup>Innovation Laboratory of Terahertz Biophysics, National Innovation Institute of Defense Technology, Beijing 100071, China<sup>2</sup>Institute of System Engineering AMS PLA Academy of Military Sciences, Beijing 100190, China<sup>3</sup>Key Laboratory of Intelligent Electromagnetic Spectrum Warfare, Beijing 100083, China<sup>4</sup>School of Physics, Peking University, Beijing 100871, China

(Received 22 October 2022; accepted 20 March 2023; published 11 May 2023)

Air-plasma is a convenient and table-top source for the broadband and coherent terahertz (THz) wave generation. However, the lack of enhancement and frequency-selecting methods for this source impedes its wide applications. Dealing with this issue, here we demonstrate a unique methodology using two spatially crossed air-plasmas. THz yields can be significantly enhanced by a factor of 7 when the two temporally overlapped THz waves are in-phase or nearly eliminated when in antiphase. This enhancement could be interpreted by using the four-wave mixing model. Meanwhile, the spectral interference of the THz amplitudes is observed and reconstructed. It enables the frequency-selectable narrow-band THz output under the suitable time delays between the two air-plasmas. These results overcome the saturation and suppression of the plasma-based THz technology and emphasize that the coherence between the THz emissions from the two filaments is a prerequisite of our methodology. Our research provides an unusual approach in enhancing and engineering the THz wave and can help to gain more insight into the mechanism of plasma-based THz generation.

DOI: [10.1103/PhysRevResearch.5.023091](https://doi.org/10.1103/PhysRevResearch.5.023091)

## I. INTRODUCTION

Laser induced air-plasma is a powerful and convenient broadband terahertz (THz) source with promising applications, e.g., the nondestructive testing [1], remote sensing [2], near-field imaging [3], ultrafast switch [4], dynamic control [5], and biodetection [6]. Generally, this source benefits from many aspects. For instance, by focusing the femtosecond laser and its second harmonic into the ambient air, molecules are ionized to form a long plasma channel (filament) and emit THz waves conveniently. In addition, the coherent THz emission covers the elusive THz frequencies, enabling a broadband-spectrum detection with high-sensitivity. Another benefit is that the plasma functions as a radiation medium that avoids the laser damage threshold to withstand a higher field strength. However, there also exists some practical challenges to the wide applications of the plasma-based THz source, especially the lack of effective approaches for its enhancement and modulation. For example, the most intuitive way to boost

the THz yield is to increase the laser input. The question is that of if the filamentation of the laser will lead to a saturation of the laser field strength, i.e., the intensity clamping [7]. Simply increasing the laser energy mainly extends the filament length and can hardly increase the plasma density [8]. Researchers observed the saturation or even suppression of the THz output when increasing the laser input energy [9,10].

Since ionization of molecules is involved in the generation process [11], plasma-based THz generation is sensitive to the spatial shape of the optical pulses as well as the formed plasmas [12,13]. Overlapping laser beams have been proposed to carve the space-time property [14] to build the plasma photonic crystal [15] and plasma grating [16–19]. This concept has been partially conducted in enhancing and engineering the THz wave by multiple filaments. Nowadays, a variety of arrangements of filaments, such as in collinear, parallel, and crossing geometries, have been extensively studied in realizing the modulation of THz waves. The collinear arrangement of two filaments can greatly suppress the THz output [20,21], which might be induced by the depletion of the neutral molecules [20] or collective absorption [22,23]. A recent study on collinearly propagating dual-color pulses and a following pulse reported a surprising enhancement of the THz outputs [24], while unfortunately it only works well under  $\mu\text{J}$ -scaled laser input and the enhancement decreases dramatically when the laser becomes intense [25]. Parallel filaments have been demonstrated to create a coherent synthesis of THz beams and to alter the emission direction [26,27]. The crossed bifilaments were shown to enhance the nonlinear interaction [16–18], generate a THz wakefield [28], vary angular and polarization properties [29], modulate the spectrum

\*Present address: Department of Physics, National University of Defense Technology, Changsha 410073, China.

<sup>†</sup>wzj0911@gmail.com

<sup>‡</sup>gwyzlzsb@pku.edu.cn

<sup>§</sup>yindonghuang@nudt.edu.cn

Published by the American Physical Society under the terms of the [Creative Commons Attribution 4.0 International](https://creativecommons.org/licenses/by/4.0/) license. Further distribution of this work must maintain attribution to the author(s) and the published article's title, journal citation, and DOI.

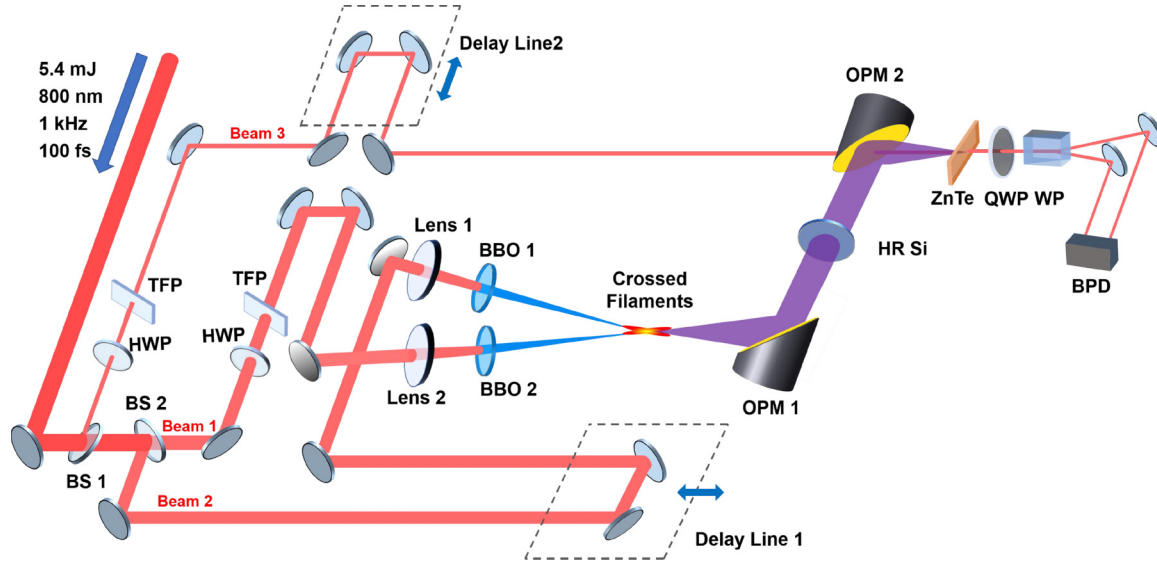


FIG. 1. (a) Schematic illustration of the experimental setup. BS 1-2: beam splitter. HWP: half-wave plate. TFP: thin film polarizers. Len 1-2: focusing lens. BBO 1-2: Type-I  $\beta$ -barium borate crystal. OPM 1-2: off-axis parabolic mirrors. HR Si: high-resistivity silicon plate. QWP: quarter-wave plate. WP: Wollaston prism. BPD: balanced photodiodes detector.

[30], and suppress the THz emissions [31,32]. These studies revealed the promising potentials of the overlapped filaments in controlling the THz wave, whereas the high laser intensity seems to place restrictions on its wide range of applications.

In this work, we demonstrate the enhancement and frequency selecting of THz emission by using two spatially crossed filaments. The intensity of THz emission from two temporally overlapped and spatially crossed filaments can be strongly enhanced by a factor of 7 when the two individual THz waves are in-phase, or nearly eliminated when they are in antiphase. This enhancement can be interpreted using the four-wave mixing (FWM) model [33]. Parallel snapshots on the filament show significantly brighter fluorescence from the temporally and spatially overlapping regions, indicating a great increase of the electron density and the plasma frequency therein. By changing the time delay between the two plasmas, the interference pattern of the THz spectra can be observed and qualitatively reconstructed. It leads to a shift of the central frequency, resulting in a frequency-selectable narrow-band THz output under suitable time delays. These results suggest that coherence between the THz emissions from the two filaments is a prerequisite of our methodology. Our findings pave an all-optical way to actively enhance and modulate the THz waves by controlling the phase and time delay between two crossed filaments.

## II. EXPERIMENTAL METHOD

### A. Experimental setup

Our experiment was performed with a Ti:sapphire laser capable of delivering 800 nm, 5.4 mJ, and 100 fs pulses at a repetition rate of 1 kHz. The experimental setup is sketched in Fig. 1. The laser pulse was split into three beams, where beams 1 and 2 both passed through a lens with a focal length of 25 cm and a 100- $\mu\text{m}$ -thick type-I  $\beta$ -barium borate (BBO) crystal. When the laser pulse is focused to ionize gaseous

molecules to produce the filament, the position of the filament will change with the incident laser energy, thereby affecting the spatial overlap of the two filaments. Therefore, we kept the incident laser energy unchanged throughout the measurement to avoid the spatial displacement of the two filaments introduced by the variety of laser intensity. The peak laser intensity of the fundamental pulse and its second harmonic was estimated to be about  $7.2 \times 10^{13} \text{ W/cm}^2$  and  $7.2 \times 10^{12} \text{ W/cm}^2$  of each input beam, respectively. The crossing angle between the two incident beams was measured to be 13 degrees. By fixing the arrangement of beam 1 and varying the light path of the delay line 1, the time delay  $t_1$  could be adjusted continuously to realize the temporal separation and coincidence of the two filaments. A high resistivity silicon plate (HR-Si) was used to block the 800-nm and 400-nm pulses and transmit the THz wave. Beam 3 was used to detect the THz waveform by electrooptic sampling (EOS) techniques. The pump-probe time delay  $t_2$  could be adjusted by moving the delay line 2. During the measurements, the fluorescence of the plasma was recorded by a charged-coupled device (CCD) placed in parallel above the filaments.

### B. Collection of the THz emissions

To collect and measure the THz wave generation from the two filaments, we used a pair of 90 degree off-axis parabolic mirrors (Thorlabs, MPD249-M01). The reflected focal length, diameter, and thickness of the parabolic mirror, all defined in Fig. 2(a), is 101.6 mm, 50.8 mm, and 62.8 mm, respectively. The numerical aperture of the parabolic mirror is calculated to be  $\sim 0.22$ . We measured the spanning angle of the THz emissions, both from each single filament and from two-crossed filaments using a Golay cell detector [34]. The spanning angle of the THz emissions from the single filament was about 5 degrees, which is in general agreement with the previous report [10]. As shown in Fig. 2(a), two sets of rays were

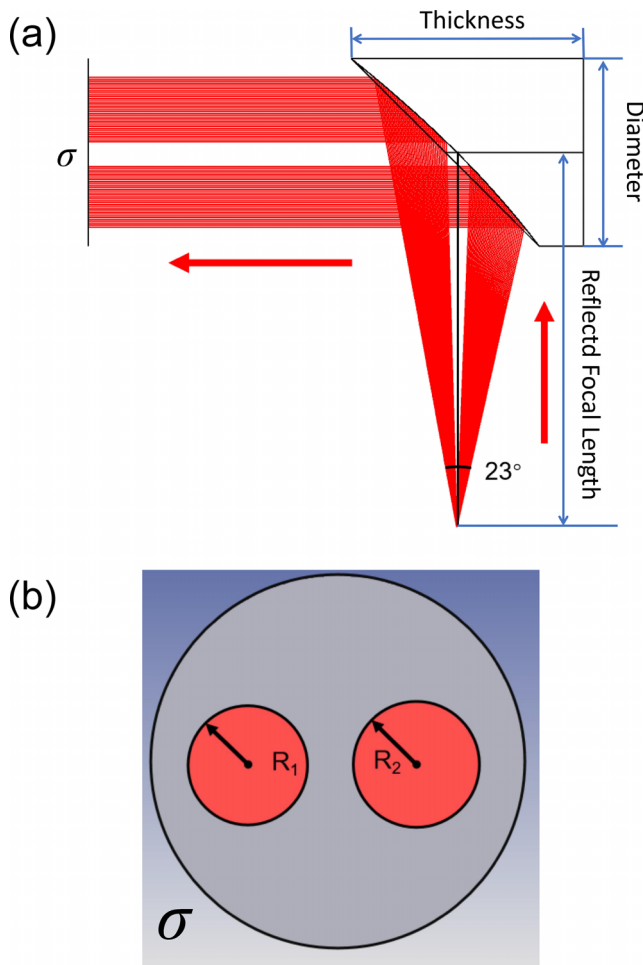


FIG. 2. (a) The propagation of two sets of rays from the focal of the parabolic mirror in the side view. The spanning angle is about 23 degrees. (b) The longitudinal profile of the two sets of rays at the surface  $\sigma$  of (a).  $R_1$  and  $R_2$  are the simulated radii of the two rays.

used to demonstrate the reflection of the THz waves radiating from two filaments through an off-axis parabolic mirror. The angle between the propagation directions of the two filaments was 13 degrees. Considering that the filaments are located at the focus of the off-axis parabolic mirror, we could simulate the propagation directions of the two sets of rays to show the propagation and collection of the THz waves in our experiment. In Fig. 2(b), we offer the longitudinal profile at the surface  $\sigma$  of Fig. 2(a), which provides the THz wave propagation (the two red areas) at the projection plane of the off-axis parabolic mirror. The simulated radius of the two THz wave beams were  $R_1 = 8.5$  mm and  $R_2 = 8.95$  mm, respectively. In addition, as was reported in our previous research [34], when the two crossed beams are overlapped in time, the propagation direction will change to being along the central line of the two laser pulses, resulting in a smaller spanning angle of the THz wave emission from the two-crossed filaments than that from two single filaments. Meanwhile, the THz wave generation from only beam 1 or beam 2 was collected by placing a screen to block the other incident beam. It helps to confirm that the off-axis parabolic mirror is capable of collecting all the THz emissions during the experiments.

### III. RESULTS AND DISCUSSIONS

#### A. Enhancement of the THz output

As shown in Fig. 3(a), we compared the snapshots of the fluorescence from two spatially crossed filaments obtained by the CCD camera for some specific time delays when  $t_1$  is  $\pm 0.8$ ,  $\pm 0.4$  and 0 ps. Obviously, when the two filaments are coincident in time ( $t_1 = 0$  ps), an extreme high-bright filament can be generated in the spatially overlapping region, denoting a considerable increase of the plasma density. To better reveal the increasing process, the integrated fluorescence intensity per millisecond versus time delay  $t_1$  is calibrated and illustrated in Fig. 3(b). When the time interval between beams 1 and 2 is more than 0.2 ps, the fluorescence intensity hardly changes with time, showing a relatively flat intensity evolution. In this case, whether beam 1 or beam 2 produces the plasma before the other, there is no observable difference in the produced fluorescence. Compared with the filament properties in Fig. 3(a), it can be found that the spatial structures of the two filaments are also almost the same at  $\pm 0.8$  ps. However, when the two light paths coincide in time, the fluorescence intensity increases sharply by a factor of about 200 times. Although the intensity of the fluorescence cannot directly correspond to the specific value of the plasma frequency, the increasing fluorescence reflects that the overlap of the two filaments can dramatically increase the electron density.

The generated THz waveforms are measured synchronously, as shown in Fig. 3(c). When the two filaments are separated in time, the sequence of the two main peaks can be clearly observed from the time domain spectra. Among them, the main peak around the time delay  $t_2 = 4$  ps is the THz waveform generated by beam 1. With the change of the time delay  $t_1$ , the THz wave that moves in the time domain is generated by beam 2. The time-domain THz wave in Fig. 3(c) presents two waveforms in sequence. An observable interaction occurs between the two waveforms, which is discussed later. It is worth noting that, when the two filaments coincide in time and space, the THz emission will be significantly enhanced.

In Fig. 3(d), we show the THz waveform and the Fourier-transformed spectra generated when the two filaments coincide in time and space. The independent THz wave generation from beams 1 and 2 are also provided in the inset for comparison. Interestingly, the measured THz amplitudes from the two crossed filaments are larger than the coherent superposition of the two distinct ones. For the two identical THz sources, if the coherent synthesis efficiency of the two reaches 100% (with no loss), the instantaneous field strength of the combined THz wave will be the coherent superposition of the two field strengths and the synthesised intensity should be four times that of the single channel [26]. However, as shown in Fig. 3(d), the THz wave intensity is enhanced by about seven times relative to the single channel.

When the two-crossed laser beams are overlapped in time, both the emitted fluorescence and the THz wave generation will exhibit a strong enhancement, while the enhancement of the first is much greater than the second. The temporally overlapped two-crossed laser beams can generate a plasma grating to greatly increase the third-order nonlinearity [16–18].

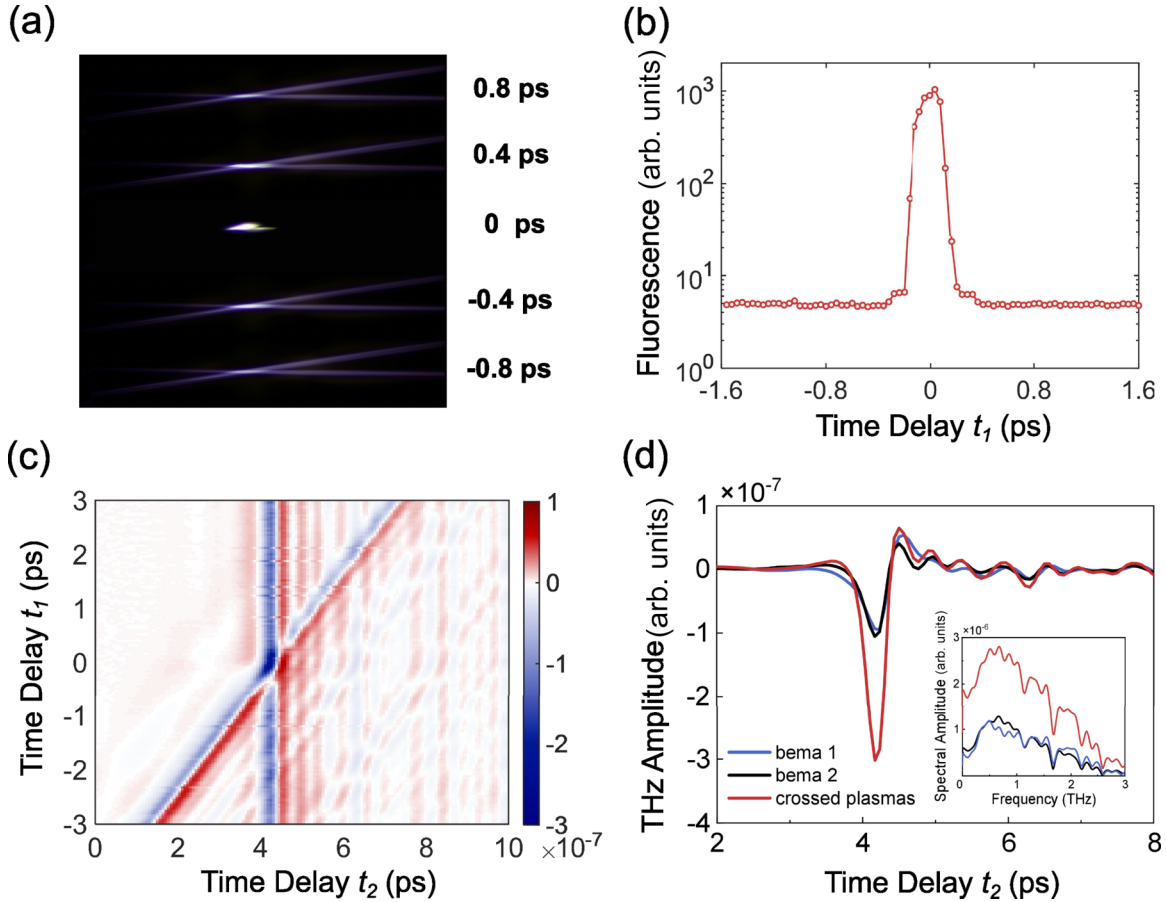


FIG. 3. (a) Snapshots of the fluorescence are obtained by the CCD camera when the time delay  $t_1$  between the two filaments is  $-0.8, -0.4, 0, 0.4, 0.8$  ps. [(b), (c)] are the experimental results of the accumulated fluorescence and THz waveform from the two crossed filaments as a function of time delay  $t_1$ . (d) Typical waveform and spectrum of the THz pulses generated from only the beam 1 (blue line), only the beam 2 (black line), and both the two beams (red line) when the time delay  $t_1 = 0$ .

Research compared the emissions between the THz wave and third-order harmonic generation from air-plasma [35]. However, the formation of the plasma grating is sensitive to the crossing angle between the two filaments [18]. In our experiment, we did not observe a significant structure of plasma grating due to the relatively large crossing angle between the two filaments.

Indeed, the enhancement of the generated THz output can be explained qualitatively using the four-wave mixing (FWM) model [33]. According to this model, the amplitude of the THz wave can be expressed as

$$E_{\text{THz}} \propto \sqrt{I_{2\omega} I_{\omega}} \cos \varphi, \quad (1)$$

where  $\varphi$  is related to the relative phase difference between the two colors,  $I_{\omega}$  and  $I_{2\omega}$  are the powers of the FW and SH, respectively. In our experiments, the powers of the incident 800 nm and 400 nm are adjusted to be the same for the two laser beams, i.e., the incident powers of the two colors are doubled in the crossed filaments. Therefore, the THz amplitude from the two filaments will be enhanced by a factor of  $2 \times \sqrt{2} \simeq 2.8$  according to Eq. (1). The corresponding THz energy yield is increased by a factor of  $2.8^2 = 7.84$  times, which is relatively close to the experimental observation. The divergence between the FWM model predictions and the

experimental measurements might be caused by an incomplete overlap between the two filaments.

It should be noted that this approach avoids the analysis of the specific electric field distribution and the interference between the two beams. Generally speaking, a femtosecond laser propagating in air results in the laser intensity clamped less than  $10^{14}$  W/cm<sup>2</sup> [36]. However, when the focusing laser energy is very high [37] or when the laser is tightly focused [8,38,39], this clamping intensity can be exceeded. Specifically, a plasma grating generated from two crossed laser beams has been reported to create an extremely high laser intensity exceeding  $4.9 \times 10^{14}$  W/cm<sup>2</sup> [17] and the corresponding intensity interference was discussed in Refs. [16–18,40]. The question is that, for the laser filamentation, the peak intensity of the two-filaments seems to be only increased by roughly 30% [41], which creates difficulty in estimating the actual field strength in plasma.

### B. Frequency selection of the THz wave

Figure 4(a) exhibits the Fourier-transformed THz spectra from the two crossed filaments under different time delays  $t_1$  in Fig. 3(c). Obviously, as we change  $t_1$  continuously, a signature of the spectral interference can be found on the frequency-dependent THz spectra. Assuming

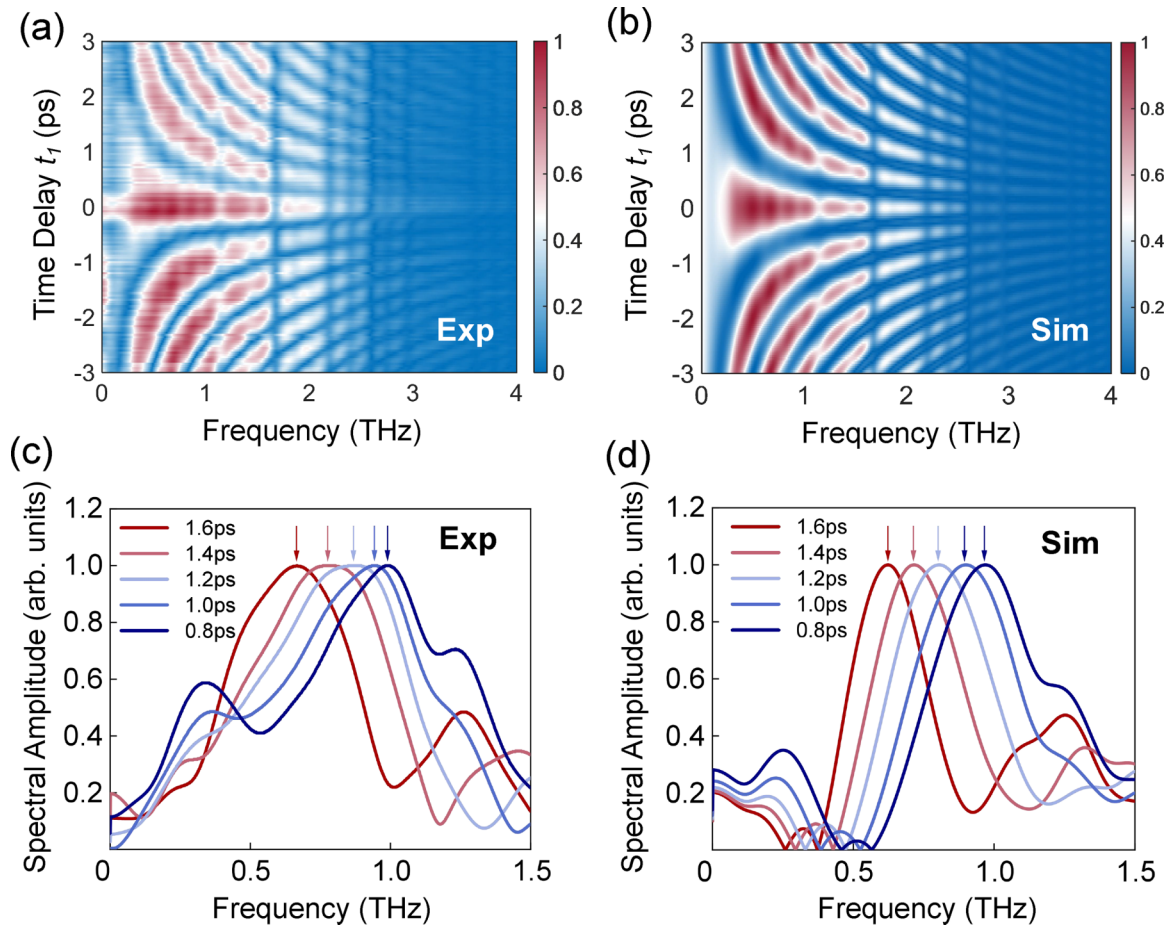


FIG. 4. [(a), (b)] are the normalized experimental and simulating results of the Fourier transformed THz amplitudes from the two in-phase crossed plasmas as a function of the time delay  $t_1$  and THz frequencies. (c) Demonstration of the frequency-selectable narrow-band THz output (normalized) when the time delay  $t_1$  is 0.8, 1.0, 1.2, 1.4, and 1.6 ps. (d) The simulation of (c).

that the THz field strength of the two filaments is  $E_{1,2}(\Omega, t) = \{E_{1,2}(\Omega) \exp(i\omega t)\}_{\text{Re}}$  with the subscripts 1 and 2 indicating the beams 1 and 2, the combined field strength  $E_{\text{com}}(\Omega, t; t_1)$  can be written as

$$E_{\text{com}}(\Omega, t; t_1) = \{[E_1(\Omega) + E_2(\Omega) \exp(i\Omega t_1 + i\Delta\phi(\Omega))] \exp(i\Omega t)\}_{\text{Re}}, \quad (2)$$

where  $\Omega$  is the THz frequency,  $t_1$  and  $\Delta\phi(\Omega)$  is the time delay and the frequency-dependent phase difference between the two THz waves.

Therefore, the frequency  $\Omega$ -dependent combined field strength from the two in-phase ( $\Delta\phi \simeq 0$ ) crossed plasmas can be further expressed as

$$E_{\text{com}}(\Omega; t_1) = E_1(\Omega) + E_2(\Omega) \cos(\Omega t_1). \quad (3)$$

By using Eq. (3) and the THz wave amplitude generated separately from the two beams, we can simulate the combined THz amplitude, as shown in Fig. 4(b). High agreement is achieved between the experimental and simulating results, and the main features of spectral interference, such as the frequencies of the maxima and minima amplitudes, are quantitatively reconstructed. The observed spectral interference demonstrates the

coherence between the two THz waves generated from the two-crossed filaments [42,43].

Due to this inherent coherence between the two THz waves, it can help to provide a frequency-selectable narrow-band THz output. It should be noted that here the output frequency is not changed or newly generated, but we just select some frequencies from the entire broadband plasma-based THz emissions. In Fig. 4(c), we demonstrate the ability of selecting the narrow-band THz radiation with a tunable central frequency from the broadband THz emissions. When the time delay  $t_1$  is tuned to be 0.8 ps, the central frequency of the spectral amplitude locates around 1 THz, and when the two beams are gradually separate to 1.6 ps in time, the central frequency shifts to 0.66 THz. In a sense, the later THz wave in a time series is somewhat like an echo of the previous one [44]. The time delay and coherence between the two THz waves ensure the elimination for some specific frequencies of THz waves. The resulting THz spectra with the time delay  $t_1$  ranging from 0.5 to 1.6 ps shows that the coherent superposition of two plasma-induced broadband THz waves can achieve a narrow-band THz output. The simulation in Fig. 4(d) reproduces this result as well.

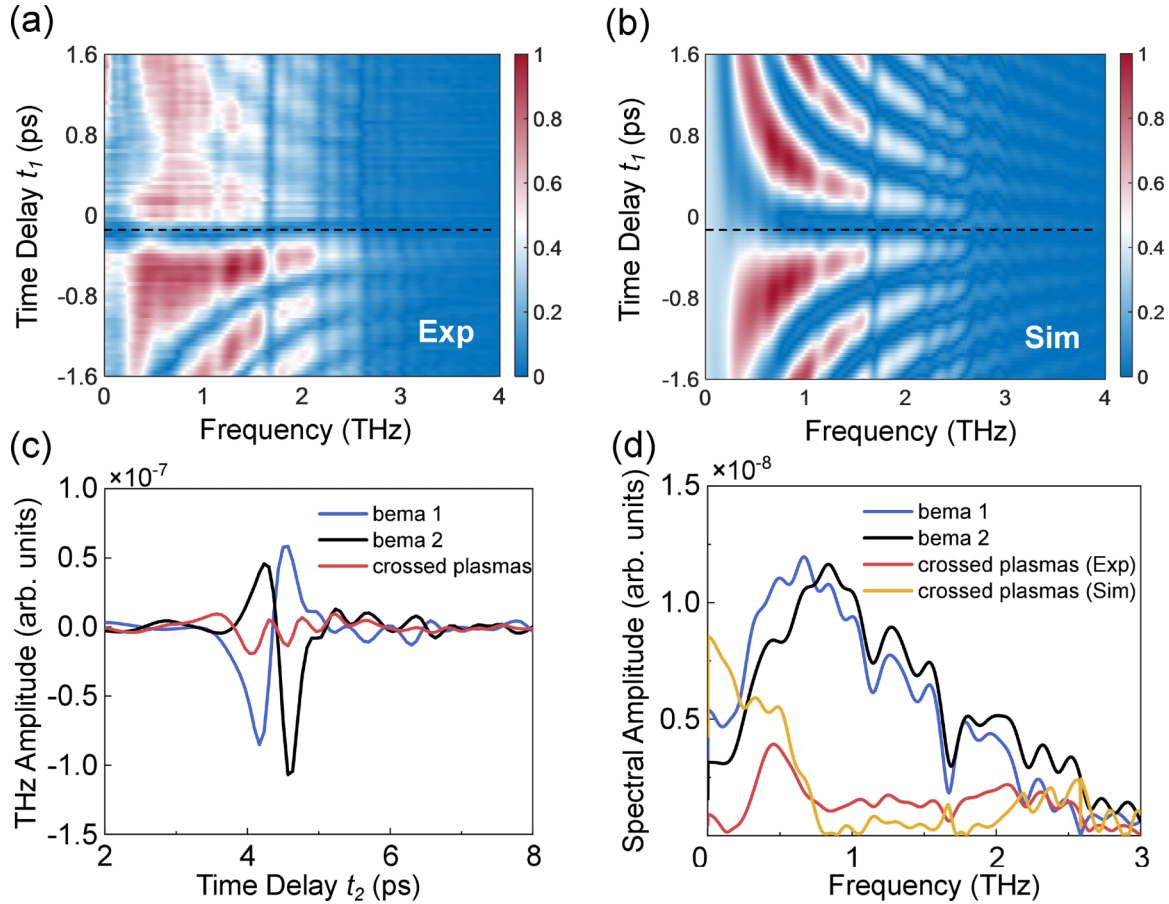


FIG. 5. [(a), (b)] are the normalized experimental and simulating results of the Fourier transformed THz amplitudes from the two crossed plasmas in antiphase as a function of the time delay  $t_1$  and THz frequencies. The black dashed lines pinpoint the dephasing time delays of the THz wave. (c) Comparisons of the THz waveforms generated from the beam 1 (blue line), the beam 2 (black line), and the two-beam generated THz waves with the antiphase (red line). (d) The Fourier transformed THz spectrums of (c) and the simulated THz wave (yellow line).

In general, any two coherent waves will have a relative-phase-dependent intensity distribution, such as the interference pattern of light emitted from two point sources. In fact, our result shares a similar concept, except that the object of the present study changes from the spatial coherence to the spectral coherence. When the two filaments are separately generating in time, the propagation direction of the two filaments and the radiated THz waves are roughly independent of each other, leading to a spectral interference of the THz wave. This result suggests that the two-crossed beams have little effect on plasma generation when they are temporally separated.

Note that there exists some discrepancy between the experimental and simulated results in Fig. 4, especially on the THz wave generation when the two crossed filaments are overlapping in time. This is because, when the two-crossed beams for THz wave generation are separated in time, the measured THz signal exhibits a spectral interference of THz pulses by the two filaments (each has a different propagation direction). However, when the two-crossed filaments overlap in time, the direction of the generated THz wave will change to mainly along the central line of the propagation directions of the two laser pulses, rather than from the two separate

filaments. The different behaviors of THz wave generation from the two-crossed filaments is determined by the time delay between beam 1 and beam 2.

### C. Antiphase-induced depletion of THz output

Next, we will show the time delay  $t_1$ -dependent Fourier-transformed THz amplitude when the two identical THz waves are in antiphase, as is illustrated in Fig. 5(a).

Experimentally, we kept the light path of beam 1 unchanged and achieved an inversion of the THz waveform from beam 2 by changing the distance from the BBO 2 crystal to the crossed filament, which introduced an additional phase between the two colors [45]. The spectral interference can also be found under different time delays of  $t_1$ , which are similar to those in Fig. 4. Following the derivation of Eq. (3), the combined field strength  $E'_{\text{com}}(\Omega)$  for the superposition of two THz waves in antiphase reads as

$$E'_{\text{com}}(\Omega) = E_1(\Omega) + E_2(\Omega) \cos(\Omega t_1 + \Delta\phi(\Omega)). \quad (4)$$

Figure 5(b) demonstrates the simulation results by using Eq. (4). Note that when  $t_1 = -0.12$  ps, the THz wave almost disappears in both the experimental result and the simulation.

We compared the experimentally generated THz waves from beam 1, beam 2, and both beams (with the time delay  $t_1$  equaling to be  $-0.12$  ps), as shown in Fig. 5(c). Interestingly, the enhancement of the THz output takes place when the time delay  $t_1$  is 0 for the in-phase THz waves' conditions, while the interference elimination of the THz radiation occurs when the time delay  $t_1$  approximates to  $-0.12$  ps in Fig. 5. The main reason for this delay between the in-phase and in antiphase results is that the position of BBO 2 has moved, resulting in the differences between the THz amplitudes [as shown in Fig. 5(d)], and the phase difference  $\Delta\phi$  does not strictly equal  $\pi$  under different frequencies. Therefore, we use the actual phase difference of  $\Delta\phi$  instead of the simple  $\pi$  in simulating the experimental results.

The previous experiments using two spatially and temporally overlapping filaments generated by one beam (800 nm) and the other of the two colors (800 nm + 400 nm) reported a frequency modulation of the THz emission, explained as a shift of the THz spectrum towards higher frequencies due to the increase in plasma density [30]. Indeed, THz emission and plasma density were found to be correlated when using the 800-nm and 400-nm scheme [46] and anticorrelated when using the 1600 nm and its second harmonic [47]. The relationship between THz generation efficiency and plasma density, depending on the wavelength of the incident light, indicates the need for a more in-depth study of the underlying generation mechanism.

In fact, fluorescence from the two-crossed filaments can be significantly enhanced when they are overlapped in time, regardless of whether the THz waves radiating from the two filaments are in phase or out of phase. This result suggests that the strength of ionization is not necessarily positively correlated with the strength of the THz waves we obtained. This could be understood using the FWM model. The phase term  $\varphi$  in Eq. (1) shares a phase difference of  $\pi$  from the

two arms of beams, resulting in an elimination of the THz emissions.

#### IV. CONCLUSION

In conclusion, we demonstrate the enhancement and central-frequency selection of THz emissions by controlling the temporal overlap between the two spatially crossed filaments. When the two crossed beams for THz wave generation are separated in time, the measured THz signal will exhibit a spectral interference of two independent THz pulses by the two filaments. While, when the two crossed beams overlap in time, the emerging plasma will generate the THz emission mainly along the central line of the two laser pulses, rather than from the two separate ones. The enhancement and elimination of the THz emissions is observed when the relative phases between the two colors in the two beams are in-phase and in antiphase, both of which could be understood based on the FWM model. The present methodology overcomes the saturation and suppression at the high laser energy input, and achieves an impressive enhancement of THz wave that exceeds the coherent synthesis efficiency, which is an instructive supplementary to the state-of-the-art plasma-based THz technology.

#### ACKNOWLEDGMENTS

This work was supported by the National Natural Science Foundation of China (Grants No. 12174449, No. 12225511, No. T2241002, and No. 61905286). C.C. acknowledges the support from the XPLORE RPRIZE. M.G. acknowledges Xi-aotong Yang of Zhejiang University for editing the language of the draft. Y.H. and M.G. acknowledges the helpful discussions with Prof. Zengxiu Zhao.

- 
- [1] S. Zhong, Progress in terahertz nondestructive testing: A review, *Front. Mech. Eng.* **14**, 273 (2019).
  - [2] J. Liu, J. Dai, S. L. Chin, and X. C. Zhang, Broadband terahertz wave remote sensing using coherent manipulation of fluorescence from asymmetrically ionized gases, *Nat. Photonics* **4**, 627 (2010).
  - [3] X.-K. Wang, J.-S. Ye, W.-F. Sun, P. Han, L. Hou, and Y. Zhang, Terahertz near-field microscopy based on an air-plasma dynamic aperture, *Light Sci. Appl.* **11**, 129 (2022).
  - [4] J. Lou, X. Xu, Y. Huang, Y. Yu, J. Wang, G. Fang, J. Liang, C. Fan, and C. Chang, Optically controlled ultrafast terahertz metadevices with ultralow pump threshold, *Small* **17**, 2104275 (2021).
  - [5] Y. Huang, J. Zhao, Z. Shu, Y. Zhu, J. Liu, W. Dong, X. Wang, Z. Lü, D. Zhang, J. Yuan, J. Chen, and Z. Zhao, Ultrafast hole deformation revealed by molecular attosecond interferometry, *Ultrafast Sci.* **2021**, 9837107 (2021).
  - [6] A. G. Markelz and D. M. Mittleman, Perspective on terahertz applications in bioscience and biotechnology, *ACS Photonics* **9**, 1117 (2022).
  - [7] S. L. Chin, S. A. Hosseini, W. Liu, Q. Luo, F. Théberge, N. Aközbebek, A. Becker, V. P. Kandidov, O. G. Kosareva, and H. Schroeder, The propagation of powerful femtosecond laser pulses in optical media: physics, applications, and new challenges, *Can. J. Phys.* **83**, 863 (2005).
  - [8] F. Théberge, W. Liu, P. T. Simard, A. Becker, and S. L. Chin, Plasma density inside a femtosecond laser filament in air: Strong dependence on external focusing, *Phys. Rev. E* **74**, 036406 (2006).
  - [9] Y. Liu, A. Houard, M. Durand, B. Prade, and A. Mysyrowicz, Maker fringes in the terahertz radiation produced by a 2-color laser field in air, *Opt. Express* **17**, 11480 (2009).
  - [10] Y. S. You, T. I. Oh, and K. Y. Kim, Off-Axis Phase-Matched Terahertz Emission from Two-Color Laser-Induced Plasma Filaments, *Phys. Rev. Lett.* **109**, 183902 (2012).
  - [11] D. Jang, R. M. Schwartz, D. Woodbury, J. Griff-McMahon, A. H. Younis, H. M. Milchberg, and K.-Y. Kim, Efficient terahertz and brunel harmonic generation from air plasma via mid-infrared coherent control, *Optica* **6**, 1338 (2019).
  - [12] F. Buccheri and X.-C. Zhang, Terahertz emission from laser-induced microplasma in ambient air, *Optica* **2**, 366 (2015).
  - [13] K. Liu, A. D. Koulouklidis, D. G. Papazoglou, S. Tzortzakis, and X.-C. Zhang, Enhanced terahertz wave emission from

- air-plasma tailored by abruptly autofocusing laser beams, *Optica* **3**, 605 (2016).
- [14] M. Rini, Carving a space-time crystal in a plasma, *Physics* **15**, s71 (2022).
- [15] X. Yang, J. Wu, Y. Peng, Y. Tong, P. Lu, L. Ding, Z. Xu, and H. Zeng, Plasma waveguide array induced by filament interaction, *Opt. Lett.* **34**, 3806 (2009).
- [16] J. Liu, W. Li, H. Pan, and H. Zeng, Two-dimensional plasma grating by non-collinear femtosecond filament interaction in air, *Appl. Phys. Lett.* **99**, 151105 (2011).
- [17] L. Shi, W. Li, Y. Wang, X. Lu, L. Ding, and H. Zeng, Generation of High-Density Electrons Based on Plasma Grating Induced Bragg Diffraction in Air, *Phys. Rev. Lett.* **107**, 095004 (2011).
- [18] Z. Liu, P. Ding, Y. Shi, X. Lu, S. Sun, X. Liu, Q. Liu, B. Ding, and B. Tao Hu, Control of third harmonic generation by plasma grating generated by two noncollinear ir femtosecond filaments, *Opt. Express* **20**, 8837 (2012).
- [19] V. R. Munirov, L. Friedland, and J. S. Wurtele, Autoresonant excitation of space-time quasicrystals in plasma, *Phys. Rev. Res.* **4**, 023150 (2022).
- [20] Y. Minami, M. Nakajima, and T. Suemoto, Effect of preformed plasma on terahertz-wave emission from the plasma generated by two-color laser pulses, *Phys. Rev. A* **83**, 023828 (2011).
- [21] J. Das and M. Yamaguchi, Terahertz wave excitation from pre-existing air plasma, *J. Opt. Soc. Am. B* **30**, 1595 (2013).
- [22] Z. Zheng, Y. Huang, Q. Guo, C. Meng, Z. Lu, X. Wang, J. Zhao, C. Meng, D. Zhang, J. Yuan *et al.*, Filament characterization via resonance absorption of terahertz wave, *Phys. Plasmas* **24**, 103303 (2017).
- [23] Y. Huang, Z. Xiang, X. Xu, J. Zhao, J. Liu, R. Wang, Z. Zhang, Z. Lü, D. Zhang, C. Chang, J. Yuan, and Z. Zhao, Localized-plasma-assisted rotational transitions in the terahertz region, *Phys. Rev. A* **103**, 033109 (2021).
- [24] S. A. Sorenson, C. D. Moss, S. K. Kauwe, J. D. Bagley, and J. A. Johnson, Enhancing terahertz generation from a two-color plasma using optical parametric amplifier waste light, *Appl. Phys. Lett.* **114**, 011106 (2019).
- [25] D. Ma, L. Dong, M. Zhang, T. Wu, Y. Zhao, L. Zhang, and C. Zhang, Enhancement of terahertz waves from two-color laser-field induced air plasma excited using a third-color femtosecond laser, *Opt. Express* **28**, 20598 (2020).
- [26] S. I. Mityukovskiy, Y. Liu, B. Prade, A. Houard, and A. Mysyrowicz, Coherent synthesis of terahertz radiation from femtosecond laser filaments in air, *Appl. Phys. Lett.* **102**, 221107 (2013).
- [27] J. Zhao, L. Guo, W. Chu, B. Zeng, H. Gao, Y. Cheng, and W. Liu, Simple method to enhance terahertz radiation from femtosecond laser filament array with a step phase plate, *Opt. Lett.* **40**, 3838 (2015).
- [28] H.-W. Du, H. Hoshina, C. Otani, and K. Midorikawa, Terahertz waves radiated from two noncollinear femtosecond plasma filaments, *Appl. Phys. Lett.* **107**, 211113 (2015).
- [29] Y. Liu, A. Houard, B. Prade, S. Akturk, A. Mysyrowicz, and V. T. Tikhonchuk, Terahertz Radiation Source in Air Based on Bifilamentation of Femtosecond Laser Pulses, *Phys. Rev. Lett.* **99**, 135002 (2007).
- [30] B. He, J. Nan, M. Li, S. Yuan, and H. Zeng, Terahertz modulation induced by filament interaction, *Opt. Lett.* **42**, 967 (2017).
- [31] Y.-S. You and K.-Y. Kim, *Terahertz Generation via Two Color Photoionization in Preformed Plasma*, in *International Conference on Ultrafast Phenomena* (Optica, Washington, D.C., 2010), p. ThE36.
- [32] T. Wu, L. Dong, S. Huang, R. Zhang, S. Zhang, H. Zhao, C. Zhang, Y. Zhao, and L. Zhang, Excitation-wavelength-dependent terahertz wave modulation via preformed air plasma, *Appl. Phys. Lett.* **112**, 171106 (2018).
- [33] X. Xie, J. Dai, and X.-C. Zhang, Coherent Control of THz Wave Generation in Ambient Air, *Phys. Rev. Lett.* **96**, 075005 (2006).
- [34] M. Gao, X. Xu, J. Lou, Z. Zhang, Z. Wen, and Y. Huang, *Terahertz Wave Generation from Crossing Air-Plasmas*, in *Terahertz Wave Generation from Crossing Air-Plasmas* (IEEE, New York, 2022), pp. 1–2.
- [35] K. Y. Kim, A. J. Taylor, J. H. Glowina, and G. Rodriguez, Coherent control of terahertz supercontinuum generation in ultrafast laser-gas interactions, *Nat. Photonics* **2**, 605 (2008).
- [36] A. Couairon and A. Mysyrowicz, Femtosecond filamentation in transparent media, *Phys. Rep.* **441**, 47 (2007).
- [37] K.-Y. Kim, J. H. Glowina, A. J. Taylor, and G. Rodriguez, High-power broadband terahertz generation via two-color photoionization in gases, *IEEE J. Quantum Electron.* **48**, 797 (2012).
- [38] P. P. Kiran, S. Bagchi, S. R. Krishnan, C. L. Arnold, G. R. Kumar, and A. Couairon, Focal dynamics of multiple filaments: Microscopic imaging and reconstruction, *Phys. Rev. A* **82**, 013805 (2010).
- [39] P. P. Kiran, S. Bagchi, C. L. Arnold, S. R. Krishnan, G. R. Kumar, and A. Couairon, Filamentation without intensity clamping., *Opt. Express* **18**, 21504 (2010).
- [40] X. Yang, J. Wu, Y. Tong, L. Ding, Z. Xu, and H. Ping Zeng, Femtosecond laser pulse energy transfer induced by plasma grating due to filament interaction in air, *Appl. Phys. Lett.* **97**, 071108 (2010).
- [41] O. G. Kosareva, W. Liu, N. A. Panov, J. Bernhardt, Z. Ji, M. Sharifi, R. F. Li, Z. Xu, J. Liu, Z. Wang, J. Ju, X. Lu, Y. Jiang, Y. X. Leng, X. Liang, V. P. Kandidov, and S. L. Chin, Can we reach very high intensity in air with femtosecond pw laser pulses? *Laser Phys.* **19**, 1776 (2009).
- [42] Z. Zhang, Y. Chen, L. Yang, X. Yuan, F. Liu, M. Chen, J. Xu, Z. Sheng, and J. Zhang, Dual-frequency terahertz emission from splitting filaments induced by lens tilting in air, *Appl. Phys. Lett.* **105**, 101110 (2014).
- [43] Y. Chen, Z. Zhang, Z. Zhang, X. Yuan, F. Liu, M. Chen, J. Xu, J. Yu, Z. Sheng, and J. Zhang, Spectral interference of terahertz pulses from two laser filaments in air, *Appl. Phys. Lett.* **106**, 221105 (2015).
- [44] S. Fleischer, R. W. Field, and K. A. Nelson, Commensurate Two-Quantum Coherences Induced by Time-Delayed THz Fields, *Phys. Rev. Lett.* **109**, 123603 (2012).
- [45] K. Y. Kim, J. H. Glowina, A. J. Taylor, and G. Rodriguez, Terahertz emission from ultrafast ionizing air in symmetry-broken laser fields, *Opt. Express* **15**, 4577 (2007).
- [46] N. Li, Y. Bai, T. Miao, P. Liu, R. Li, and Z. Xu, Revealing plasma oscillation in thz spectrum from laser plasma of molecular jet, *Opt. Express* **24**, 23009 (2016).
- [47] Z. Yu, L. Sun, N. Zhang, J. Wang, P. Qi, L. Guo, Q. Sun, W. Liu, and H. Misawa, Anti-correlated plasma and thz pulse generation during two-color laser filamentation in air, *Ultrafast Sci.* **2022**, 9853053 (2022).